

UC Santa Barbara

UC Santa Barbara Previously Published Works

Title

Manipulating the ABCs of self-assembly via low- χ block polymer design

Permalink

<https://escholarship.org/uc/item/9gj7k2qp>

Journal

Proceedings of the National Academy of Sciences of the United States of America, 114(25)

ISSN

0027-8424

Authors

Chang, Alice B
Bates, Christopher M
Lee, Byeongdu
et al.

Publication Date

2017-06-20

DOI

10.1073/pnas.1701386114

Peer reviewed

Manipulating the ABCs of self-assembly via low- χ block polymer design

Alice B. Chang^a, Christopher M. Bates^{b,c,1}, Byeongdu Lee^d, Carol M. Garland^e, Simon C. Jones^f, Russell K. W. Spencer^{g,h,i}, Mark W. Matsen^{g,h,i,1}, and Robert H. Grubbs^{a,1}

^aArnold and Mabel Beckman Laboratories for Chemical Synthesis, California Institute of Technology, Pasadena, CA 91125; ^bMaterials Department, University of California, Santa Barbara, CA 93106; ^cDepartment of Chemical Engineering, University of California, Santa Barbara, CA 93106; ^dX-Ray Science Division, Advanced Photon Source, Argonne National Laboratory, Argonne, IL 60439; ^eDepartment of Materials Science, California Institute of Technology, Pasadena, CA 91125; ^fElectrochemical Technologies Group, Jet Propulsion Laboratory, California Institute of Technology, Pasadena, CA 91109; ^gDepartment of Chemical Engineering, University of Waterloo, Waterloo, ON N2L 3G1, Canada; ^hDepartment of Physics & Astronomy, University of Waterloo, Waterloo, ON N2L 3G1, Canada; and ⁱWaterloo Institute for Nanotechnology, University of Waterloo, Waterloo, ON N2L 3G1, Canada

Contributed by Robert H. Grubbs, May 7, 2017 (sent for review January 25, 2017; reviewed by Thomas Epps and Edwin L. Thomas)

Block polymer self-assembly typically translates molecular chain connectivity into mesoscale structure by exploiting incompatible blocks with large interaction parameters (χ_{ij}). In this article, we demonstrate that the converse approach, encoding low- χ interactions in ABC bottlebrush triblock terpolymers ($\chi_{AC} \lesssim 0$), promotes organization into a unique mixed-domain lamellar morphology, which we designate LAM_p. Transmission electron microscopy indicates that LAM_p exhibits ACBC domain connectivity, in contrast to conventional three-domain lamellae (LAM₃) with ABCB periods. Complementary small-angle X-ray scattering experiments reveal a strongly decreasing domain spacing with increasing total molar mass. Self-consistent field theory reinforces these observations and predicts that LAM_p is thermodynamically stable below a critical χ_{AC} above which LAM₃ emerges. Both experiments and theory expose close analogies to ABA' triblock copolymer phase behavior, collectively suggesting that low- χ interactions between chemically similar or distinct blocks intimately influence self-assembly. These conclusions provide fresh opportunities for block polymer design with potential consequences spanning all self-assembling soft materials.

block polymer | self-assembly | polymer nanostructure | domain spacing | LAM_p

Block polymers are a diverse class of soft materials capable of self-assembling into complex periodic nanostructures. Synthetic command over composition, dispersity, sequence, and molecular architecture enables control over the mesoscopic order and macroscopic thermal, mechanical, rheological, and transport properties (1–4). The phase behavior of “simple” linear AB diblock copolymers is universally parameterized by the segregation strength $\chi_{AB}N$ and relative volume fraction f , where χ_{AB} represents the effective Flory–Huggins binary interaction parameter and N is the total volume-averaged degree of polymerization. Mixing behavior, captured through the mean-field concept of χ_{AB} , is central to block polymer self-assembly: the competing demands of minimizing interfacial energy and maximizing configurational entropy only favor microphase separation when A–B interactions are repulsive ($\chi_{AB} > 0$) (5, 6). Extension to higher-order multiblock polymers introduces additional interaction parameters (χ_{ij}) that impact self-assembly and properties (7). For example, introducing a mutually incompatible C block ($\chi_{AC} > 0$, $\chi_{BC} > 0$) generates a host of new morphologies dictated by the chain connectivity (ABC, ACB, or BAC) and intrinsic χ_{ij} -values (8, 9). In this rich phase space, designing multiblock polymers with a combination of miscible and immiscible blocks can also access new structures and impart useful functions (10, 11). Perhaps the best-known examples of such systems are linear ABA' triblock copolymers ($\chi_{AB} > 0$, $\chi_{AA'} \approx 0$); their high-value industrial applications as thermoplastic elastomers are entirely enabled by A/A' mixing and chain connectivity, which together create physically cross-linked materials with excellent processability and mechanical properties (12). The self-assembly of yet more complex systems, including ABA'C tetrablock polymers (13, 14) and

$A_n(BA'_m)$ heteroarm star polymers (15), is also crucially determined by A/A' miscibility. These examples illuminate interesting parallels and contrasts between block polymer phase behavior and protein self-assembly. Nature delivers exquisite control over protein folding by precisely tailoring amino acid sequences and intramolecular interactions that are often attractive (e.g., hydrogen bonding), whereas block polymer design to date exploits simple molecular connectivity and primarily repulsive interactions ($\chi > 0$) to induce microphase separation.

Previous reports have investigated the role of negligible ($\chi \sim 0$) or attractive ($\chi < 0$) intermolecular interactions on the phase behavior of various homopolymer (AB/A') (16, 17) and block polymer (AB/A'C) (18, 19) blends. In contrast, studies in which the macromolecules themselves are intramolecularly encoded with miscible blocks are to the best of our knowledge limited to the aforementioned A/A' self-similar interactions. In this report, we study ABC bottlebrush triblock terpolymers with grafted poly(D,L-lactide), poly(styrene), and poly(ethylene oxide) side chains (LSO), featuring low- χ interactions ($\chi_{AC} \lesssim 0$) between distinct A and C end blocks. These materials generate a unique mixed morphology with atypical mesoscopic domain connectivity, which we denote LAM_p. Additionally, under certain conditions of molecular asymmetry, another consequence of low- χ design manifests in decreasing domain spacing with increasing total molar mass.

Significance

Molecular sequence and interactions dictate the mesoscale structure of all self-assembling soft materials. Block polymers harness this relationship to access a rich variety of nanostructured materials but typically require energetically unfavorable (high- χ) interactions between blocks. Contrary to this convention, we demonstrate that ABC triblock terpolymers featuring low- χ interactions between end blocks can self-assemble into a unique mixed morphology that subverts the demands of chain connectivity. As a consequence of block–block mixing, the characteristic length scales of these self-assembled structures exhibit an unusual trend: As the total polymer size increases, the domain spacing decreases. These developments expand the vocabulary of block polymer design and open additional avenues for manipulating the self-assembly of synthetic macromolecules.

Author contributions: A.B.C., C.M.B., and R.H.G. designed research; A.B.C., S.C.J., R.K.W.S., and M.W.M. performed research; A.B.C., B.L., C.M.G., S.C.J., R.K.W.S., and M.W.M. contributed new reagents/analytic tools; A.B.C., C.M.B., B.L., and M.W.M. analyzed data; R.H.G. directed and served as principal investigator and discussed interpretation of the results; and A.B.C. and C.M.B. wrote the paper.

Reviewers: T.E., University of Delaware; and E.L.T., Rice University.

The authors declare no conflict of interest.

¹To whom correspondence may be addressed. Email: bates@enr.ucsb.edu, mwmatson@uwaterloo.ca, or rhg@caltech.edu.

This article contains supporting information online at www.pnas.org/lookup/suppl/doi:10.1073/pnas.1701386114/-DCSupplemental.

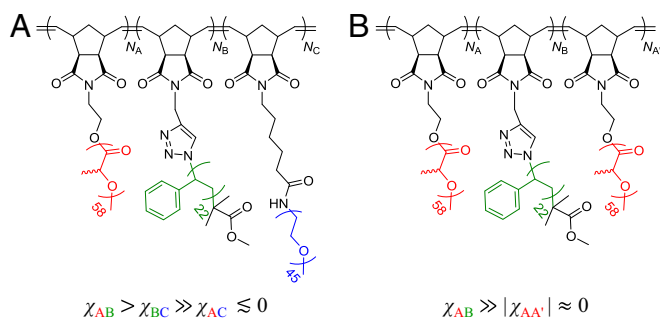


Fig. 1. Molecular structures and relative interaction parameters for (A) LSO and (B) LSL' brush triblock polymers.

Valuable insight into the molecular origins of this unusual behavior is achieved by comparison with analogous ABA' brush triblock copolymers—grafted poly(_{D,L}-lactide)-*block*-poly(styrene)-*block*-poly(_{D,L}-lactide) (LSL')—and self-consistent field theory (SCFT). The experimental and theoretical conclusions described herein regarding low- χ block polymers reveal unexpected breadth in self-assembly and should create new opportunities for molecular and materials design.

Results and Discussion

Synthesis and Structure of Low- χ Block Polymers. ABC and ABA' brush triblock polymers containing grafted poly(_{D,L}-lactide) (PLA, A block), polystyrene (PS, B block), and poly(ethylene oxide) (PEO, C block) side chains were synthesized by ring-opening metathesis polymerization (ROMP) (20–22). The living nature and synthetic utility of ROMP enable the formation of well-defined block polymers with precisely controlled molar mass, narrow molar mass dispersity, and diverse pendant functionalities. Synthetic details (SI Appendix, Scheme S1), characterization data (SI Appendix, Tables S1 and S2), and size-exclusion chromatograms (SI Appendix, Figs. S1–S3) for all samples are provided. Fig. 1 illustrates the molecular structure of the LSO and LSL' brush triblock polymers studied herein and highlights the relative interaction parameters dictated by block chemistry and sequence. Both LSO and LSL' feature low- χ interactions between the end blocks ($\chi_{AC}, \chi_{AA'} \lesssim 0$), which in particular distinguish LSO from typical frustrated ABC triblock polymers that include similar relative χ -values but highly unfavorable A/C interactions ($\chi_{AC} \gg 0$) (9, 23). $N_A, N_B,$ and (N_C or $N_{A'}$) indicate the number-average degrees of polymerization through the polynorbornene backbone for blocks containing PLA, PS, and (PEO or PLA) grafts, respectively. All LSO and LSL' triblock polymers were annealed at 140 °C under modest applied pressure, and the ordered structures that developed were identified by synchrotron small-angle X-ray scattering (SAXS) (e.g., see SI Appendix, Fig. S4).

SCFT. SCFT, generally regarded as the state of the art for block polymer melts (24), was used to model our polymers and provide insight into their self-assembly. The standard model for branched polymers was modified to account for the strong steric interactions that occur in bottlebrushes due to the high grafting density of the side chains, as was done previously for similar bottlebrush block polymers (25). Gaussian chains were used to represent the $N = N_A + N_B + N_C$ (LSO) or $N = N_A + N_B + N_{A'}$ (LSL') side chains, and the volumes and unperturbed end-to-end lengths of the side chains were set to known literature values (26, 27). For the backbone, a worm-like chain of fixed persistence length was used to handle the strong lateral tension that occurs due to side-chain crowding. The interactions between the three side-chain species (PLA, PS, and PEO) were represented in the Hamiltonian by standard Flory–Huggins terms controlled by $\chi_{LS}, \chi_{SO},$ and χ_{LO} . The equilibrium lamellar period (d^*) was obtained by minimizing the free energy (F). Additional SCFT details,

including values for all parameters (SI Appendix, Table S3) and a schematic of chain dimensions (SI Appendix, Scheme S2), are provided.

Unique Domain Connectivity. We begin by presenting data and calculations corresponding to LSO brush triblock terpolymers (Fig. 1A), then draw close analogies to LSL' (Fig. 1B) phase behavior. All LSO materials self-assemble into well-ordered lamellar morphologies. Transmission electron micrographs of thin sections of LSO* ($N_A = 28, N_B = 27, N_C = 5$) stained over ruthenium tetroxide (RuO_4) vapor reveal a three-color, four-layer lamellar morphology (Fig. 2A). (Additional images are provided in the SI Appendix, Fig. S5.) Exposing L, S, and O to RuO_4 vapor results in unstained, slightly stained, and strongly stained domains, respectively, as deduced from literature results: PS is selectively stained in PLA/PS mixtures (28, 29), and PEO is stained to a greater extent than PS (30, 31). Surprisingly, the extent of staining and layer widths observed by transmission electron microscopy (TEM) are completely inconsistent with both the side-chain volume fractions measured by ^1H NMR ($f_L = 0.57, f_S = 0.37, f_O = 0.06$) (Fig. 2B) and the ABCB connectivity required by the expected three-domain microstructure, LAM_3 (Fig. 2C) (8, 9). The conflict between LAM_3 and the pattern observed by TEM can only be resolved by invoking partial mixing between the A and C end blocks, apparently driven by low- χ interactions ($\chi_{AC} \lesssim 0$). The resulting morphology exhibits mesoscopic ACBC connectivity (Fig. 2D), consistent with the observed staining pattern. Because the three blocks are not well-segregated, the side-chain volume fractions are not required to equal the relative domain widths. Reflecting the crucial role of partial mixing, this unique morphology is herein designated LAM_P .

SCFT fully supports the distinction between LAM_3 (Fig. 3A) and LAM_P (Fig. 3B), controlled primarily by the relative and absolute interaction parameters. Composition profiles for LSO* were calculated over one lamellar period using realistic PLA–PS ($\chi_{AB} \equiv \chi_{LS}$) and PS–PEO ($\chi_{BC} \equiv \chi_{SO}$) values estimated in the literature: $\chi_{LS} = 0.080$ (32) and $\chi_{SO} = 0.049$ (33) at 140 °C, renormalized to a common monomer reference volume (118 \AA^3). (We note that literature χ -values obtained by fitting experimental data to mean-field approximations are often inaccurate, potentially affecting the agreement between experiment and theory (34).) PLA–PEO interactions ($\chi_{AC} \equiv \chi_{LO}$) were arbitrarily varied in the simulations, and LAM_3 is correctly predicted to occur at moderate to large χ_{AC} (Fig. 3C), in broad agreement with previous experimental and theoretical studies of frustrated ABC triblock terpolymers (35–37). In contrast, LAM_P exclusively emerges when χ_{AC} is sufficiently small to favor partial A/C block–block mixing (Fig. 3D). Using this collection of physical parameters, a first-order phase transition between LAM_3 and

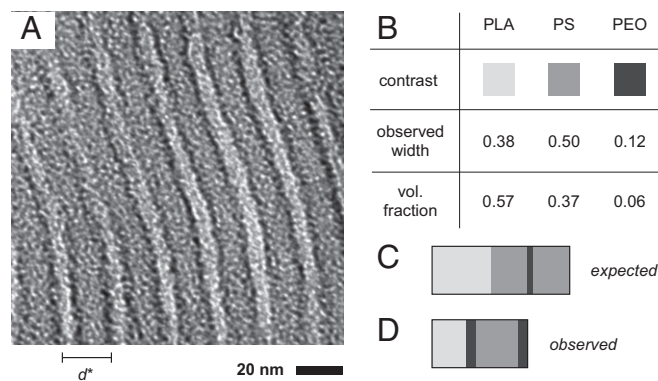


Fig. 2. (A) TEM of LSO* stained with RuO_4 . (B) Relative contrast from the stain, relative widths of corresponding layers observed by TEM, and side-chain volume fractions measured by ^1H NMR. (C) One LAM_3 period with the expected ABCB domain connectivity and layer widths based on data in B. (D) One LAM_P period observed in A, exhibiting mesoscopic ACBC domain connectivity.

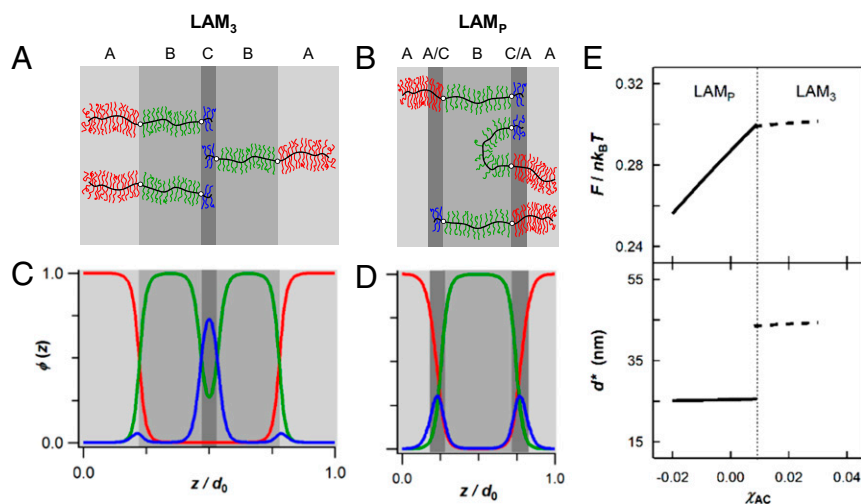


Fig. 3. Illustrations and SCFT data distinguishing LAM₃ and LAM_P morphologies. In A–D, the light-, medium-, and dark-gray layers represent PLA, PS, and PEO (or mixed PLA/PEO) domains, respectively. (A and B) LSO chain packing in (A) LAM₃ and (B) LAM_P. (C and D) SCFT composition profiles for LSO* within one normalized lamellar period (z/d_0), where $\phi(z)$ is the relative segment concentration of each component. (C) $\chi_{AC} > \chi^C$: LAM₃ with $d^* = 43.5$ nm. (D) $\chi_{AC} < \chi^C$: LAM_P with $d^* = 25.6$ nm. (E) SCFT calculations of the normalized free energy (*Top*) and domain spacing (*Bottom*) versus $\chi_{AC} \equiv \chi_{LO}$ for LSO*. The transition from mixed (LAM_P) to unmixed (LAM₃) morphologies is first order, occurring at a critical value χ^C (dotted line); for $\chi_{AB} = 0.080$ and $\chi_{BC} = 0.049$, $\chi^C = 0.009$.

LAM_P was predicted to occur at a critical value $\chi^C = 0.009$ (Fig. 3E). The mesoscopic ACBC domain connectivity and relative domain widths predicted for LAM_P perfectly match the pattern observed in Fig. 2A and reinforce the microscopic origins of mixing deduced from TEM.

Decreasing Domain Spacing with Increasing Total Molar Mass. A series of LSO brush triblock terpolymers with fixed $N_A = 26$ and $N_B = 24$ (guaranteed by a common parent diblock) and variable

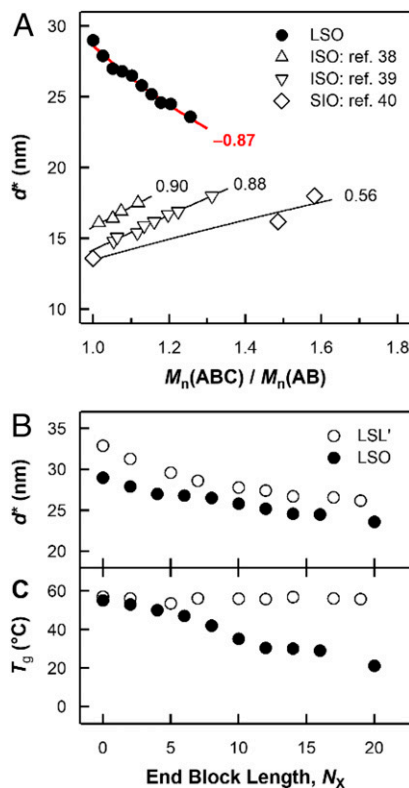


Fig. 4. (A) Lamellar periods (d^*) versus normalized molar mass for brush LSO (this work) and linear ISO and SIO triblock terpolymers (literature data). Calculated exponents (best fit) to the power law $d^* \sim M^x$ are included for comparison. (B and C) Consequences of varying end-block length N_x in LSL' and LSO. (B) Domain spacing d^* . (C) Apparent PLA glass transition temperatures (T_g); for all samples, a single T_g ($T_{g,PEO} < T_g \leq T_{g,PLA}$) was observed.

N_C (SI Appendix, Scheme S3) highlights additional consequences of block–block mixing. N_C was varied in increments of two or four backbone repeat units, from $N_C = 0$ (LSO-0) to $N_C = 20$ (LSO-20) (SI Appendix, Table S1). (Note that, due to the high molar mass of each PEO macromonomer, the total molar mass varies by >45,000 g/mol across this series.) SAXS measurements reveal an unusual trend: as the total molar mass (M) increases over the range of compositions where LAM_P forms ($0 < f_O \leq 0.20$), the lamellar period (d^*) strongly decreases: $d^* \sim M^{-0.87}$ (Fig. 4A). For comparison, Fig. 4A also includes literature data for linear poly(isoprene-*b*-styrene-*b*-ethylene oxide) (ISO) and poly(styrene-*b*-isoprene-*b*-ethylene oxide) (SIO) triblock terpolymers similarly synthesized by varying the O block length from a common parent diblock. The domain spacing trends observed for both ISO and SIO series typify the expected increase in lamellar period with increasing M : $\alpha_{ISO} \approx 0.90$ (38, 39) and $\alpha_{SIO} \approx 0.56$ (40). Clearly, α_{LSO} is strikingly different. Additional data illustrating the unusual negative trend for LSO are summarized in the SI Appendix, Table S4. Schematic illustrations of assigned structures (SI Appendix, Fig. S6), indexed 2D SAXS data (SI Appendix, Fig. S7), 1D azimuthally averaged intensity reductions (SI Appendix, Fig. S8), and TEM images (SI Appendix, Fig. S9) are also provided.

A series of LSL' brush triblock copolymers was similarly synthesized from identical macromonomers, generating an analogous series with variable end-block length from a parent LS diblock ($N_A = 30$, $N_B = 28$). Like LSO, this LSL' series exhibits decreasing lamellar periods with increasing end-block length (i.e., increasing total molar mass) (Fig. 4B). Additional morphological data for LSL' are provided in the SI Appendix, Table S5 and Figs. S10 and S11. Differential scanning calorimetry data for LSL' and LSO are compared in Fig. 4C and provide quantitative evidence of block–block mixing in LSO. For all LSO samples, a single glass transition temperature (T_g) was observed between $T_{g,PLA}$ (55 °C) and $T_{g,PEO}$ (–70 °C) (SI Appendix, Fig. S12). As N_C (and therefore the weight fraction of PEO) increases, T_g decreases, consistent with continued dilution of mixed A/C domains by the low- T_g component. The presence of only one T_g in polymer blends is generally regarded as evidence for miscibility (41, 42) and is consistent with the behavior of PLA and PEO homopolymers, which mix over wide ranges of molar masses and blend compositions (43, 44). In the analogous LSL' series, a single T_g corresponding to the PLA block is observed that does not change as N_A increases, because mixed domains inherently remain pure PLA (SI Appendix, Fig. S13).

Role of Low- χ Interactions. We have investigated herein the impact of low- χ block–block interactions on structure and physical properties by studying densely grafted ABC and ABA' brush triblock polymers. The LSO polymers described above self-assemble into lamellae with unique domain connectivity (ACBC), which we denote LAM_P. In

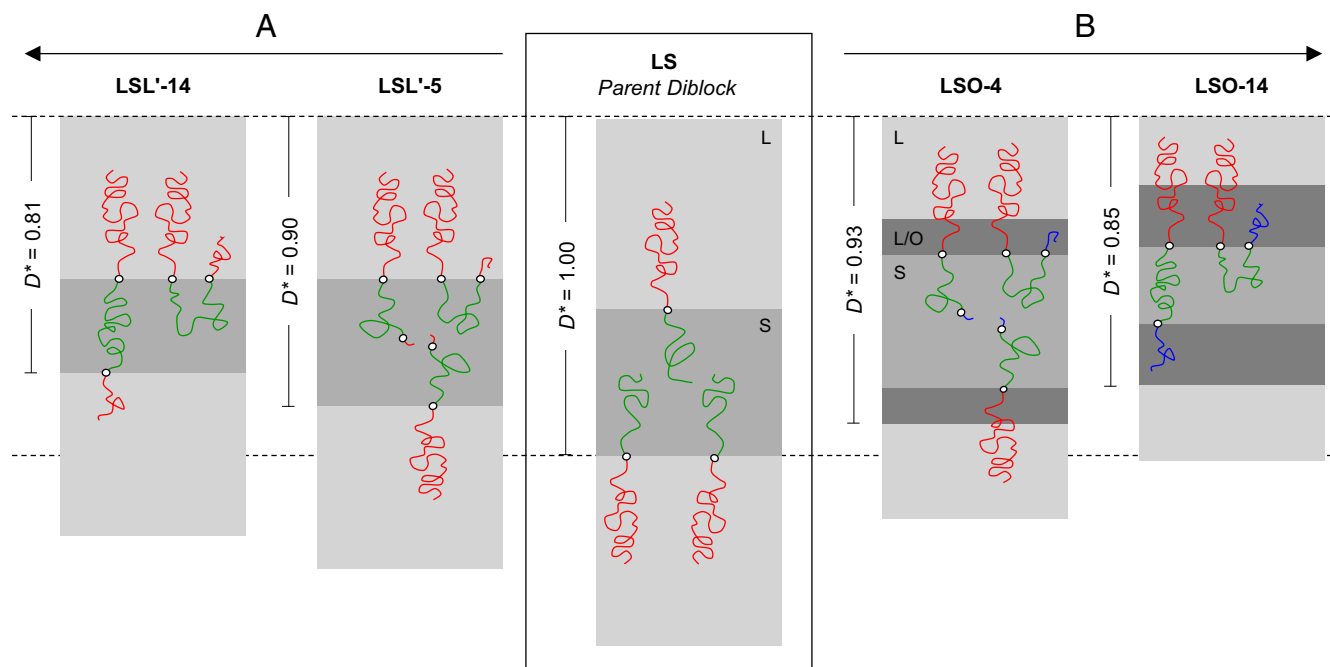


Fig. 5. Illustration of chain pullout to explain the trends in d^* for LSL' and LSO brush triblock polymers with varying end-block length (equivalently, varying molecular asymmetry). Linear chains are depicted to aid visualization. As the end-block length N_x increases from a fixed parent LS diblock, d^* decreases (here, $D^* \equiv d^*/d^*_{LS}$, where d^*_{LS} is the period of the parent LS diblock). (A) $X = A'$ (LSL'): short PLA end blocks pull out of PLA domains into PS domains. (B) $X = C$ (LSO): short PEO end blocks pull out of mixed PLA/PEO domains into PS domains.

responsible for the unusual trend in d^* : Whereas both LSO and LSL' exhibit decreasing d^* with increasing end-block lengths, LSL' has no crystallizable components.

We expect that the phenomena described above, illustrating the physical consequences of designing polymers with certain miscible blocks, are general to the class of soft materials with $\chi_{AB}, \chi_{BC} \gg |\chi_{AC}| \approx 0$. Although bottlebrush polymers were used in the present study, SCFT calculations predict identical behavior for analogous linear triblock terpolymers with the same absolute and relative χ -parameters (*SI Appendix, Fig. S17*). Although bottlebrush polymers experience some steric-induced stiffening compared to linear polymers (58, 59), our results suggest that brush LSO and LSL' are actually relatively flexible. The backbone flexibility should enable brush LS(O/L') to adopt looping midblock configurations (Figs. 3 and 5), just like linear AB(C/A') triblocks with compatible end blocks (60, 61). Informed SCFT calculations indicate that the effective backbone persistence length of brush LSO and LSL' corresponds to ~ 5 norbornene repeat units (25). Because the B midblocks of LSO and LSL' are much longer than 5 units ($N_B \geq 24$), they should readily form loops, although undoubtedly less than the 40% predicted for flexible (linear) triblocks (62). Our results, placed in the context of recent work on bottlebrush block polymer self-assembly, suggest that polymer architecture is not a major factor controlling the formation of partially mixed morphologies. Instead, the primary driving force appears to be the magnitude of χ_{AC} . Designed low- χ interactions emerge as tools to manipulate block polymer self-assembly.

Potential Nonequilibrium Behavior. Although SCFT calculations suggest that LAM_P is at equilibrium with experimentally relevant values of χ and f , experimental proof is currently limited by our inability to access the order–disorder transition temperature (T_{ODT}). SAXS data obtained upon heating a LAM_P sample (LSO with $N_A = 25, N_B = 22, N_C = 5$) from 25 to 200 °C indicate that LAM_P is thermally stable throughout the entire experimentally accessible temperature range (*SI Appendix, Fig. S18*). Consistent with other reports of high-molar-mass bottlebrush polymers (25, 63), no T_{ODT} is observed below the onset of decomposition, preventing

careful annealing and quench studies originating from the disordered state. Because SCFT is an equilibrium theory, any deviations from equilibrium would affect the agreement between experimentally measured results and predicted behavior.

To further probe potential nonequilibrium effects and because morphologies for multiblock polymers can be sensitive to processing conditions (64, 65), an LSO brush triblock terpolymer ($N_A = 25, N_B = 22, N_C = 5$) was annealed in four different ways: thermal annealing under pressure, thermal annealing without pressure, drop casting, and channel die alignment. All approaches afforded self-assembled morphologies with virtually identical LAM_P geometry and periodicity (± 0.5 nm) (*SI Appendix, Fig. S19*). These results are reported while acknowledging studies of linear multiblock polymers that highlight the potential influence of processing path on the formation of kinetically trapped structures (66, 67), which may be mistaken for equilibrium. Previously, ABC block polymer morphologies containing partially mixed regions have indeed been predicted (68) and observed (69) as metastable defect states kinetically trapped upon casting from preferential solvents, but these examples were easily annihilated during the type of extended thermal treatments performed herein to anneal LSO. Equilibrium or not, the morphological attributes of LAM_P are long-lived, in contrast to and notably distinct from prior materials.

Conclusion

The insights gained herein from both experiment and theory illustrate the profound influence low- χ interactions exert on self-assembly. Proper selection of χ_{ij} and f can generate unusual morphologies characterized by partial block mixing (LAM_P), decouple molecular sequence from mesoscopic connectivity, and provide counterintuitive control over domain spacing. Whereas high- χ block polymers have been the subject of widespread interest, low- χ systems remain relatively unexplored, yet the latter generate fascinating physics that are anticipated to gain importance as sequence complexity further evolves. Expanding the block polymer design toolkit to include low- χ interactions creates new opportunities to tailor mesoscale structure and should find utility in the future design of functional materials.

ACKNOWLEDGMENTS. The authors thank M. S. Ladinsky for assistance with ultramicrotomy, as well as M. T. Irwin, S. Chanpuriya, and T. Li for helpful discussions about sample preparation and TEM. The authors gratefully acknowledge helpful discussions with F. S. Bates and Z.-G. Wang. This work was supported by the National Science Foundation through Grant CHE-1502616. A.B.C. thanks the US Department of Defense for support through

the National Defense Science and Engineering Graduate (NDSEG) Fellowship. C.M.B. thanks the Dreyfus Foundation for Environmental Postdoctoral Fellowship EP-13-142 and the University of California, Santa Barbara for funding. This research used resources of the Advanced Photon Source, a US Department of Energy Office of Science User Facility operated by Argonne National Laboratory under Contract DE-AC02-06CH11357.

- Thomas EL (1999) The ABCs of self-assembly. *Science* 286:1307.
- Park C, Yoon J, Thomas EL (2003) Enabling nanotechnology with self assembled block copolymer patterns. *Polymer (Guildf)* 44:6725–6760.
- Lutz J-F, Ouchi M, Liu DR, Sawamoto M (2013) Sequence-controlled polymers. *Science* 341:1238149.
- Bates CM, Bates FS (2016) 50th anniversary perspective: Block polymers—pure potential. *Macromolecules* 50:3–22.
- Leibler L (1980) Theory of microphase separation in block copolymers. *Macromolecules* 13:1602–1617.
- Bates FS, Fredrickson GH (1999) Block copolymers—designer soft materials. *Phys Today* 52:32–38.
- Bates FS, et al. (2012) Multiblock polymers: Panacea or Pandora's box? *Science* 336:434–440.
- Zheng W, Wang Z-G (1995) Morphology of ABC triblock copolymers. *Macromolecules* 28:7215–7223.
- Bailey TS (2001) Morphological behavior spanning the symmetric AB and ABC block copolymer states. PhD thesis (University of Minnesota, Minneapolis).
- Xie N, et al. (2014) Macromolecular metallurgy of binary mesocrystals via designed multiblock terpolymers. *J Am Chem Soc* 136:2974–2977.
- Gao Y, Deng H, Li W, Qiu F, Shi A-C (2016) Formation of nonclassical ordered phases of AB-type multiarm block copolymers. *Phys Rev Lett* 116:068304.
- Legge NR (1987) Thermoplastic elastomers. *Rubber Chem Technol* 60:83–117.
- Bluemle MJ, Zhang J, Lodge TP, Bates FS (2010) Inverted phases induced by chain architecture in ABAC tetrablock terpolymers. *Macromolecules* 43:4449–4452.
- Lee S, Bluemle MJ, Bates FS (2010) Discovery of a Frank-Kasper σ phase in sphere-forming block copolymer melts. *Science* 330:349–353.
- Lynd NA, Oyerokun FT, O'Donoghue DL, Handlin DL, Fredrickson GH (2010) Design of soft and strong thermoplastic elastomers based on nonlinear block copolymer architectures using self-consistent-field theory. *Macromolecules* 43:3479–3486.
- Hashimoto T, Tanaka H, Hasegawa H (1990) Ordered structure in mixtures of a block copolymer and homopolymers. 2. Effects of molecular weights of homopolymers. *Macromolecules* 23:4378–4386.
- Matsen MW (1995) Phase behavior of block copolymer/homopolymer blends. *Macromolecules* 28:5765–5773.
- Kimishima K, Jinnai H, Hashimoto T (1999) Control of self-assembled structures in binary mixtures of A–B diblock copolymer and A–C diblock copolymer by changing the interaction between B and C block chains. *Macromolecules* 32:2585–2596.
- Tang C, et al. (2010) Multiple nanoscale templates by orthogonal degradation of a supramolecular block copolymer lithographic system. *ACS Nano* 4:285–291.
- Sveinbjörnsson BR, et al. (2012) Rapid self-assembly of brush block copolymers to photonic crystals. *Proc Natl Acad Sci USA* 109:14332–14336.
- Bates CM, Chang AB, Momčilović N, Jones SC, Grubbs RH (2015) ABA triblock brush polymers: Synthesis, self-assembly, conductivity, and rheological properties. *Macromolecules* 48:4967–4973.
- Bates CM, et al. (2016) Brush polymer ion gels. *J Polym Sci, B, Polym Phys* 54:292–300.
- Radlauer MR, et al. (2016) Morphological consequences of frustration in ABC triblock polymers. *Macromolecules* 50:446–458.
- Fredrickson GH (2006) *The Equilibrium Theory of Inhomogeneous Polymers* (Oxford Univ Press, New York).
- Dalsin SJ, et al. (2015) Bottlebrush block polymers: Quantitative theory and experiments. *ACS Nano* 9:12233–12245.
- Fetters LJ, Lohse DJ, Richter D, Witten TA, Zirkel A (1994) Connection between polymer molecular weight, density, chain dimensions, and melt viscoelastic properties. *Macromolecules* 27:4639–4647.
- Dorgan JR, et al. (2005) Fundamental solution and single-chain properties of poly-lactides. *J Polym Sci, B, Polym Phys* 43:3100–3111.
- Olayo-Valles R, Lund MS, Leighton C, Hillmyer MA (2004) Large area nanolithographic templates by selective etching of chemically stained block copolymer thin films. *J Mater Chem* 14:2729–2731.
- Vayer M, Nguyen TH, Sinturel C (2014) Ruthenium staining for morphological assessment and patterns formation in block copolymer films. *Polymer (Guildf)* 55:1048–1054.
- Trent JS, Scheinbeim JI, Couchman PR (1983) Ruthenium tetroxide staining of polymers for electron microscopy. *Macromolecules* 16:589–598.
- Gai Y, Song D-P, Yavitt BM, Watkins JJ (2017) Polystyrene-block-poly(ethylene oxide) bottlebrush block copolymer morphology transitions: Influence of side chain length and volume fraction. *Macromolecules* 50:1503–1511.
- Zalusky AS, Olayo-Valles R, Wolf JH, Hillmyer MA (2002) Ordered nanoporous polymers from polystyrene-poly(lactide) block copolymers. *J Am Chem Soc* 124:12761–12773.
- Cochran EW, Morse DC, Bates FS (2003) Design of ABC triblock copolymers near the ODT with the random phase approximation. *Macromolecules* 36:782–792.
- Beardsley TM, Matsen MW (2016) Universality between experiment and simulation of a diblock copolymer melt. *Phys Rev Lett* 117:217801.
- Stadler R, et al. (1995) Morphology and thermodynamics of symmetric poly(A-block-B-block-C) triblock copolymers. *Macromolecules* 28:3080–3097.
- Balsamo V, et al. (2003) Morphological behavior of thermally treated polystyrene-*b*-polybutadiene-*b*-poly(ϵ -caprolactone) ABC triblock copolymers. *Macromolecules* 36:4515–4525.
- Liu M, Li W, Qiu F, Shi A-C (2012) Theoretical study of phase behavior of frustrated ABC linear triblock copolymers. *Macromolecules* 45:9522–9530.
- Bailey TS, Hardy CM, Epps TH, Bates FS (2002) A noncubic triply periodic network morphology in poly(isoprene-*b*-styrene-*b*-ethylene oxide) triblock copolymers. *Macromolecules* 35:7007–7017.
- Meuler AJ, et al. (2009) Polydispersity effects in poly(isoprene-*b*-styrene-*b*-ethylene oxide) triblock terpolymers. *J Chem Phys* 130:234903.
- Bailey TS, Pham HD, Bates FS (2001) Morphological behavior bridging the symmetric AB and ABC states in the poly(styrene-*b*-isoprene-*b*-ethylene oxide) triblock copolymer system. *Macromolecules* 34:6994–7008.
- Couchman PR (1978) Compositional variation of glass-transition temperatures. 2. Application of the thermodynamic theory to compatible polymer blends. *Macromolecules* 11:1156–1161.
- Gaikwad AN, Wood ER, Ngai T, Lodge TP (2008) Two calorimetric glass transitions in miscible blends containing poly(ethylene oxide). *Macromolecules* 41:2502–2508.
- Younes H, Cohn D (1988) Phase separation in poly(ethylene glycol)/poly(lactic acid) blends. *Eur Polym J* 24:765–773.
- Sheth M, Kumar RA, Davé V, Gross RA, McCarthy SP (1997) Biodegradable polymer blends of poly(lactic acid) and poly(ethylene glycol). *J Appl Polym Sci* 66:1495–1505.
- Sioula S, Hadjichristidis N, Thomas EL (1998) Novel 2-dimensionally periodic non-constant mean curvature morphologies of 3-miktoarm star terpolymers of styrene, isoprene, and methyl methacrylate. *Macromolecules* 31:5272–5277.
- Tang P, Qiu F, Zhang H, Yang Y (2004) Morphology and phase diagram of complex block copolymers: ABC star triblock copolymers. *J Phys Chem B* 108:8434–8438.
- Frielinghaus H, et al. (2001) Micro- vs. macro-phase separation in binary blends of poly(styrene)-poly(isoprene) and poly(isoprene)-poly(ethylene oxide) diblock copolymers. *Europhys Lett* 53:680–686.
- Chatterjee J, Jain S, Bates FS (2007) Comprehensive phase behavior of poly(isoprene-*b*-styrene-*b*-ethylene oxide) triblock copolymers. *Macromolecules* 40:2882–2896.
- Mao H, Hillmyer MA (2008) Morphological behavior of polystyrene-block-poly(lactide)/polystyrene-block-poly(ethylene oxide) blends. *Macromol Chem Phys* 209:1647–1656.
- Lai W-C, Liao W-B, Lin T-T (2004) The effect of end groups of PEG on the crystallization behaviors of binary crystalline polymer blends PEG/PLLA. *Polymer (Guildf)* 45:3073–3080.
- Matsen MW (2000) Equilibrium behavior of asymmetric ABA triblock copolymer melts. *J Chem Phys* 113:5539–5544.
- Milner ST, Witten TA (1988) Bending moduli of polymeric surfactant interfaces. *J Phys France* 49:1951–1962.
- Hammersky MW, Smith SD, Gozen AO, Spontak RJ (2005) Phase behavior of triblock copolymers varying in molecular asymmetry. *Phys Rev Lett* 95:168306.
- Smith SD, Hammersky MW, Bowman MK, Rasmussen KO, Spontak RJ (2006) Molecularly asymmetric triblock copolymers as a single-molecule route to ordered bidisperse polymer brushes. *Langmuir* 22:6465–6468.
- Winey KI, Thomas EL, Fetters LJ (1991) Swelling of lamellar diblock copolymer by homopolymer: Influences of homopolymer concentration and molecular weight. *Macromolecules* 24:6182–6188.
- Koizumi S, Hasegawa H, Hashimoto T (1994) Spatial distribution of homopolymers in block copolymer microdomains as observed by a combined SANS and SAXS method. *Macromolecules* 27:7893–7906.
- Chen S-C, Kuo S-W, Jeng US, Su C-J, Chang F-C (2010) On modulating the phase behavior of block copolymer/homopolymer blends via hydrogen bonding. *Macromolecules* 43:1083–1092.
- Fredrickson GH (1993) Surfactant-induced lyotropic behavior of flexible polymer solutions. *Macromolecules* 26:2825–2831.
- Mikhaylov IV, Darinskii AA (2015) Effect of the side-arm architecture on the conformational properties of bottle brushes. *Polym Sci Ser A* 57:239–250.
- Zhulina EB, Halperin A (1992) Lamellar mesogels and mesophases: A self-consistent-field theory. *Macromolecules* 25:5730–5741.
- Kane L, Spontak RJ (1994) Microstructural characteristics of strongly-segregated AXB triblock terpolymers possessing the lamellar morphology. *Macromolecules* 27:1267–1273.
- Matsen MW, Thompson RB (1999) Equilibrium behavior of symmetric ABA triblock copolymer melts. *J Chem Phys* 111:7139–7146.
- Xia Y, Olsen BD, Kornfield JA, Grubbs RH (2009) Efficient synthesis of narrowly dispersed brush copolymers and study of their assemblies: The importance of side chain arrangement. *J Am Chem Soc* 131:18525–18532.
- Mori K, Hasegawa H, Hashimoto T (1990) Ordered structure in block polymer solutions. 6. Possible non-equilibrium effects on growth of self-assembling structures. *Polymer (Guildf)* 31:2368–2376.
- Lodge TP, Pudil B, Hanley KJ (2002) The full phase behavior for block copolymers in solvents of varying selectivity. *Macromolecules* 35:4707–4717.
- Lipic PM, Bates FS, Matsen MW (1999) Non-equilibrium phase behavior of diblock copolymer melts and binary blends in the intermediate segregation regime. *J Polym Sci, B, Polym Phys* 37:2229–2238.
- Chanpuriya S, et al. (2016) Cornucopia of nanoscale ordered phases in sphere-forming tetrablock terpolymers. *ACS Nano* 10:4961–4972.
- Xia J, Sun M, Qiu F, Zhang H, Yang Y (2005) Microphase ordering mechanisms in linear ABC triblock copolymers. A dynamic density functional study. *Macromolecules* 38:9324–9332.
- Corté L, et al. (2003) Annealing and defect trapping in lamellar phases of triblock terpolymers. *Macromolecules* 36:7695–7706.